

Heterogeneous & Homogeneous & Bio- & Nano-

CHEM **CAT** CHEM

CATALYSIS

Accepted Article

Title: Comprehensive understanding the role of Brønsted and Lewis acid sites in glucose conversion to 5-hydroxymethylfurfural

Authors: Yanqin Wang, Xiangcheng Li, Kaihao Peng, Xiaohui Liu, and Qineng Xia

This manuscript has been accepted after peer review and appears as an Accepted Article online prior to editing, proofing, and formal publication of the final Version of Record (VoR). This work is currently citable by using the Digital Object Identifier (DOI) given below. The VoR will be published online in Early View as soon as possible and may be different to this Accepted Article as a result of editing. Readers should obtain the VoR from the journal website shown below when it is published to ensure accuracy of information. The authors are responsible for the content of this Accepted Article.

To be cited as: *ChemCatChem* 10.1002/cctc.201601203

Link to VoR: <http://dx.doi.org/10.1002/cctc.201601203>

WILEY-VCH

www.chemcatchem.org



Comprehensive understanding the role of Brønsted and Lewis acid sites in glucose conversion to 5-hydroxymethylfurfural

Xiangcheng Li, Kaihao Peng, Xiaohui Liu*, Qineng Xia, Yanqin Wang*^[a]

Abstract: In this paper, the conversion of glucose and the selectivity to 5-hydroxymethylfurfural (HMF) are investigated over various silica-alumina composite (AlSiO) catalysts. The type, amount and strength of the acidic sites were characterized by NH₃-TPD and Py-FTIR techniques, and then correlated with the catalytic conversion of glucose to HMF for providing a quantitative relationship between the acidity and products selectivity. The results showed that Lewis acid sites played important role in glucose conversion, which can enhance the isomerization of glucose to fructose, while Brønsted acid sites had detrimental effect on glucose conversion. Very importantly, it is shown that the HMF selectivity had a nearly linear relationship with the weak/total Lewis acid (L*/L) ratio, indicating that the weak Lewis acid could promote the formation of HMF. Further analysis showed that the medium to strong Lewis acid sites can enhance the formation of the undesired by-products (levulinic acid, humins). It is also found that the B/L ratio had an influence on HMF selectivity, at every similar L*/L ratio, volcano curves were obtained with the increase of B/L ratio, but the change was not as great as the influence of L*/L ratio. Furthermore, niobium incorporated Nb-AlSiO catalysts were prepared and used in the conversion of glucose to HMF, which also confirmed the above findings. Under optimized conditions, HMF selectivity can reach as high as 71% at 92.6% conversion of glucose and no obvious decline after four catalytic cycles.

Introduction

An unprecedented international effort has been made to explore alternative renewable lignocellulosic biomass for the large-scale production of fuels and chemicals due to the rapid depletion of fossil fuels. 5-Hydroxymethylfurfural (HMF), derived from C6 carbohydrates, is one of the most versatile and important building blocks, because it can be upgraded into a large number of chemicals.^[1]

HMF is formed by the loss of three water molecules from a hexose by acid catalysis. It can be easily obtained from fructose by using a wide variety of homogeneous and heterogeneous catalysts,^[2] but fructose is produced from glucose in industry catalyzed by enzyme, making glucose a more desirable substrate. Glucose can be converted to HMF via a tandem steps: first glucose is isomerized to fructose in the presence of an enzyme, a Lewis acid or base catalyst,^[3,4] then fructose is

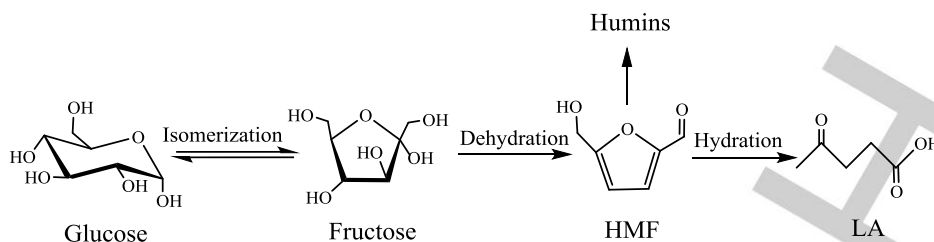
dehydrated to HMF. During these processes, side reactions always accompany, such as the further hydration of HMF to levulinic acid and the polymerization of HMF itself or with fructose to humins.^[5] These reaction pathways are drawn in scheme 1. The unwanted reactions have been identified as the main obstacle for the production of HMF commercially from glucose, so the selective conversion of glucose to HMF represents currently one of the key challenges in biorefining processes. Understanding the reaction of glucose conversion and controlling the side reactions is a big challenge. To overcome this challenge, many groups have explored the mechanism for the isomerization of glucose and dehydration of fructose to HMF.^[4,6-10]

Vlachos et al.^[6] investigated the mechanisms of glucose isomerization in aqueous media over various Lewis acids, metal(III) chlorides, and found that the metal chlorides isomerized glucose to fructose via a C2–C1 intramolecular hydride transfer. Recently, elucidating how the surface acidities of solid acid catalysts work on the Lewis acid-catalyzed glucose isomerization reaction has received much attention. A key development in glucose isomerization by heterogeneous catalytic systems was made by Davis and co-workers, it was well established that the Sn-beta was an effective Lewis acid catalyst for the glucose isomerization to fructose.^[4] Furthermore, Bell et al.^[7] investigated the isomerization mechanism consisting of a sequence of ring-opening, isomerization, and ring-closing processes over metal substituted beta zeolite and it was found the Sn and Zr which acted as Lewis acid sites showed the low reaction barrier for glucose isomerization.

Ordonsky et al.^[8] found high selectivity to HMF (55–60%) was achieved over silylated phosphates, due to a decrease in the amount of Lewis acidity which would lead to unselective glucose transformation into humins, and the selectivity to HMF increased with the increase of B/L ratio (ca. 0.09–0.27). But this result was conflicted with our previous work^[10] that the selectivity to HMF decreased with the increase of B/L ratio (ca. 0.72–1.85) over NbPO catalysts. Then, a recent study showed that HMF formation rate exhibited volcano type curve vs. the B/L ratio, and the maximum HMF yield approached 60% was achieved in biphasic phase.^[9] The above reports indicated that the Lewis acid sites played important role in the isomerization of glucose, and the HMF selectivity had correlation with B/L ratio; but at best of our knowledge, no clear correlations between the types and strength of acid sites with products selectivity had been reported.

It was shown recently that mesoporous silica-alumina composite (AlSiO) could catalyze the glucose conversion to HMF efficiently.^[11] Here, the conversion of glucose and the selectivity to HMF are well correlated with the acidic properties of various silica-alumina composite (AlSiO) catalysts, which offered a possibility for deeply understanding the nature of the active sites on glucose isomerization, dehydration reactions and

[a] X.C. Li, K. H. Peng, Dr. X.H. Liu, Dr. Q.N. Xia, Prof. Y. Q. Wang
Shanghai Key Laboratory of Functional Materials Chemistry and
Research Institute of Industrial Catalysis, School of Chemistry and
Molecular Engineering
East China University of Science and Technology
No. 130 Meilong Road, Shanghai (PR China)
Fax: (+86)21-64253824
E-mail: xhliu@ecust.edu.cn; wangyanqin@ecust.edu.cn



Scheme 1. The reaction pathway for the conversion of glucose to HMF.

further for the design of catalysts. Moreover, we continue our study to investigate the acidic properties of AlSiO by modifying with niobium and further verify the findings on glucose conversion.

Results and Discussion

Characterization of texture properties and surface acidity of AlSiO and NbPO catalysts

A series of AlSiO catalysts were prepared by a sol-gel method as described before^[11] and modified with post-treatments (silylation, ionic-exchange). The NbPO-pH2 and Al-NbPO-pH2 catalysts were also used for expanding the scope of acidity. The X-ray powder diffraction patterns of AlSiO-20, AlSiO-10, AlSiO-20/B, AlSiO-20/L, Na-AlSiO-20, NbPO-pH2 and Al-NbPO-pH2 catalysts are shown in Figure 1. It can be seen that all the AlSiO samples are amorphous, as only one broad band is detected from $2\theta = 15^\circ$ to 40° for each sample, which implies the amorphous characteristic of these materials. NbPO-2 and Al-NbPO-2 samples display two broad peaks in the 2θ range of $15-40^\circ$ and $40-60^\circ$, indicating the amorphous characteristic and no crystallized NbPO or Nb₂O₅ phase are detected.

The acidic properties of different catalysts were investigated by temperature-programmed desorption of ammonia and the

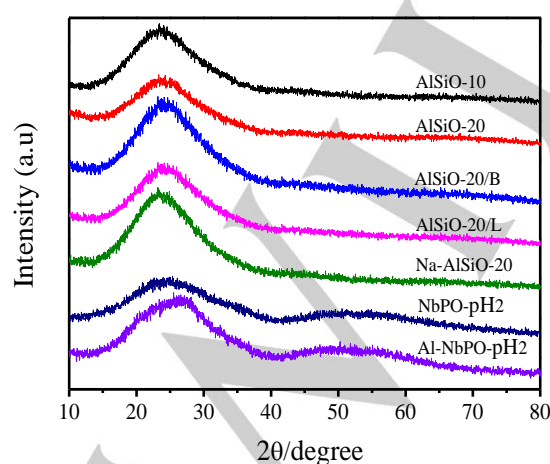


Figure 1. XRD patterns of various catalysts.

results are plotted in Figure 2. The AlSiO samples (except for Na-AlSiO-20 sample) and NbPO samples exhibited the ammonia desorption at two temperatures: a low-temperature peak at 180°C and a high-temperature peak at $300-500^\circ\text{C}$, corresponding to the weak and medium to strong acid sites. For Na-AlSiO-20, the peak is rather narrow and concentrated at 180°C , indicating its weak acidity. The total amounts of the acid sites determined by NH₃-TPD increases in the following order: Na-AlSiO-20 < AlSiO-20 < AlSiO-20/B < AlSiO-20/L < AlSiO-10, and the total acid sites of NbPO-2 is close to that of Al-NbPO-2.

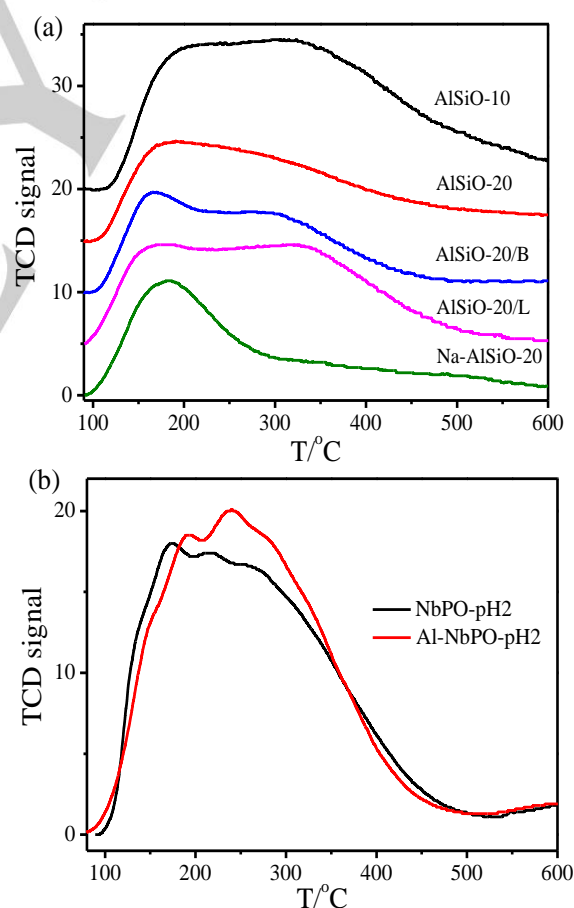
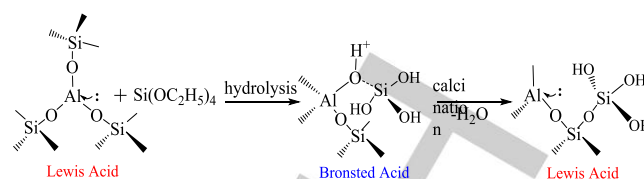


Figure 2. NH₃-TPD profiles of various catalysts. (a) AlSiO and (b) NbPO samples. (The TCD signal of AlSiO-20/L, AlSiO-20/B, AlSiO-20, AlSiO-10 shifted up 5, 10, 15, 20, respectively).

To investigate the different types and strength of acidic sites on various catalysts, the Py-FTIR spectra were recorded at different temperatures and drawn in Figure S1. The intense bands at 1448 cm^{-1} and 1540 cm^{-1} are due to Lewis and Brønsted acid sites, respectively, and the band at 1490 cm^{-1} is attributed to the adsorption of pyridine on both Brønsted and Lewis acid sites.^[12] The weak sites are defined as the ones from which pyridine is removed by evacuation at between 100 °C and 200 °C , the medium strength corresponds to evacuation between 200 °C and 400 °C and the strong sites remains adsorbing pyridine after evacuation at 400 °C .

Table 1 summarized the concentration of the Lewis and Brønsted acid sites calculated on the basis of the extinction coefficients from bands at 1448 cm^{-1} and 1540 cm^{-1} , respectively, at different temperature. The intensity of the band assigned to pyridine adsorbed on Brønsted acid sites increases in the following order: Na-AISiO-20 < AISiO-20 < AISiO-20/L < AISiO-10 \approx AISiO-20/B < Al-NbPO-pH2 < NbPO-pH2. In order to reduce Brønsted acid sites, AISiO-20 catalyst was treated with NaOH and resulted in a significant decrease in the amount of Brønsted acid sites from 106 to $40\text{ }\mu\text{mol g}^{-1}$ (Na-AISiO-20 catalyst, Table 1). While treatment of the AISiO-20 with TEOS (AISiO-20/B) leads to a significant increase in the amount of Brønsted acid sites and decrease in the Lewis acid sites, this procedure is well known for deactivation of acid sites on the external surface of zeolites.^[13,14] Lewis acid sites were located at the external surface, thus, having a higher accessibility for TEOS compared to the bridging hydroxyl groups,^[14] the introducing of silanol groups and bridging hydroxyl groups which came from new Si-O-Al bonds formed led to the increase of Brønsted acid sites on the surface (Scheme 2).



Scheme 2. Possible mechanism of deactivation Brønsted and Lewis acid sites formation by silylation over silica-alumina composite.

The intensity of the band assigned to pyridine adsorbed on Lewis acid sites increases in the following order: AISiO-20/B < Na-AISiO-20 \approx NbPO-pH2 < AISiO-20 \approx Al-NbPO-pH2 < AISiO-20/L < AISiO-10. The AISiO-20/L catalyst was obtained by calcining AISiO-20/B catalyst at 550 °C , resulting in the increase of Lewis acid sites ($550\text{ }\mu\text{mol g}^{-1}$) with a low effect on the Brønsted acid sites (Table 1), a possible explanation is the loss of bridging hydroxyl groups and silanol groups after calcination (Scheme 2), then more three-coordinated Al atoms formed which acted as Lewis acid sites by accepting the lone pair of electrons. Doping aluminium in NbPO-pH2 can enhance Lewis acid because aluminium is always considered as a strong Lewis acid site. As shown in Table 1 and Figure S1, the Lewis acid sites increased from 346 to $469\text{ }\mu\text{mol g}^{-1}$, which indicates that aluminium is indeed a good strong Lewis acid center. In summarize, we have prepared several catalysts which contain various strength of acid with different B/L acid ratio, following the glucose dehydration over these catalysts are investigated and discussed in the next section.

Table 1. Surface area and amounts of Brønsted and Lewis acid sites on various catalysts by Py-FTIR.

Entry	Cata	$S_{\text{BET}}/\text{m}^2\text{g}^{-1}$	Acid from Py-FTIR ($\mu\text{mol g}^{-1}$)											
			Brønsted				Lewis				Total	B/L	B*/B	L*/L
			W	M	S	Total	W	M	S	Total				
1	AISiO-20	717.6	12	14	80	106	151	185	81	417	523	0.26	0.11	0.35
2	AISiO-10	722.9	102	129	66	297	172	362	104	638	935	0.47	0.34	0.27
3	AISiO-20/B	360.4	81	132	124	337	125	67	75	267	604	1.27	0.24	0.47
4	AISiO-20/L	662.0	37	83	112	232	44	385	121	550	782	0.30	0.16	0.08
5	Na-AISiO-20	360.4	19	10	11	40	180	41	95	316	357	0.13	0.48	0.57
6	NbPO-pH2	290.1	77	241	323	641	69	242	35	346	986	1.86	0.12	0.20
7	Al-NbPO-pH2	50.4	122	136	234	492	32	119	318	469	962	1.05	0.25	0.07
8 ^[a]	AISiO-10	-	102	129	535	766	172	362	104	638	1404	1.20	0.13	0.27
9 ^[b]	AISiO-20/B	-	81	132	124	337	125	67	309	501	838	0.67	0.24	0.25
10 ^[c]	Al-NbPO-pH2	-	122	136	414	672	32	119	318	469	1141	1.43	0.18	0.07

W: weak acid sites; M: medium acid sites; S: strong acid sites;

B*/B: weak / total Brønsted acid sites;

L*/L: weak / total Lewis acid sites;

0.2g catalyst added: [a] 2 ml 0.05 mol/L HCl; [b] 30 mg yttrium(III) triflate; [c] 2 ml 0.02 mol/L HCl.

Effect of the acidity on the conversion of glucose

The conversion of glucose and the selectivity to HMF, levulinic acid and humins during dehydration of glucose over various catalysts are investigated and all data are collected in Table 2. Besides the main products were detected in the reaction system by HPLC. Fructose was not detected and the selectivity to furfural was below 1 mol %. Humins could not be observed by HPLC or GC-MS, therefore the amount of humins produced was estimated from the carbon balance.

The conversion of glucose over various catalysts increased in the order: AlSiO-20/B < Na-AlSiO-20 < NbPO-pH2 < AlSiO-20 < Al-NbPO-pH2 < AlSiO-20/L < AlSiO-10, this order did not correspond to the increase of the total amounts of acid sites. As shown in Figure S2, the glucose conversion exhibited a volcano curve with the total amounts of acid sites, it initially increased with the total acidity, then decreased slightly when the total acidity was larger than $935 \mu\text{mol g}^{-1}$.

Further detailed analysis showed that glucose conversion also exhibited a volcano relationship with the Brønsted acid sites (Figure S2), suggesting that more Brønsted acid sites might suppress glucose conversion, which agreed with our previous results over NbOPO4 catalysts.^[10] To further verify this, AlSiO-10 sample with additional Brønsted acid, such as hydrochloric acid was used to evaluate this reaction under the same conditions (Table 2, Entry 8) and found that it really decreased the conversion of glucose from 98.9% to 90.9%, which confirmed that Brønsted acid sites had detrimental effect on the glucose isomerization process. Then for AlSiO-20/B sample, which had similar Brønsted acid sites ($337 \mu\text{mol g}^{-1}$) to that of AlSiO-10 sample ($297 \mu\text{mol g}^{-1}$), but lower glucose conversion (68.6%) was obtained than that (98.8%) over AlSiO-10 sample

(Table 2, Entry 2,3), this might due to the more Lewis acid sites of AlSiO-10 sample, which would promote glucose conversion.

Further analysis showed a positive correlation between glucose conversion and Lewis acid sites (Figure 4), meaning that Lewis acid sites really promoted glucose conversion since glucose isomerization was a Lewis acid catalyzed reaction.^[4,10] This was further confirmed by using AlSiO-20/B sample with additional Lewis acid, Yttrium trifluoroacetate $[(\text{TfO})_3\text{Y}]$ to evaluate this reaction under the same conditions (Table 2, Entry 11), it was indeed found that glucose conversion increased from 68.6% to 92.4%. The above findings showed that Lewis acid sites played important role in the glucose conversion via isomerization of glucose into fructose, whereas Brønsted acid sites had detrimental effect on this isomerization process.

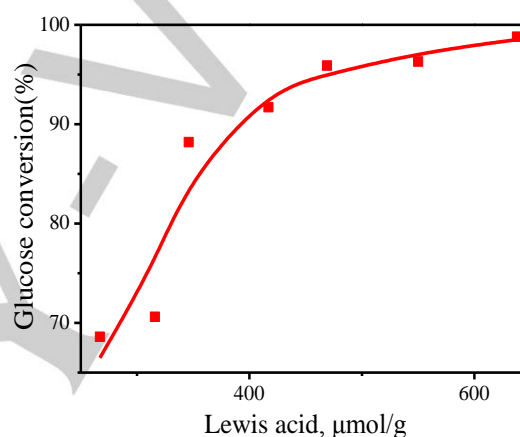


Figure 4. Effect of the Lewis acid sites on the conversion of glucose over various catalysts under the same reaction condition.

Table 2. Summary of the glucose conversion, HMF yield and selectivity, LA yield and selectivity and humins selectivity catalyzed by various catalysts.

Entry	Catalyst	C_{glucose} /%	Y_{HMF} /%	Y_{LA} /%	S_{HMF} /%	S_{LA} /%	S_{humins} /%
1	AlSiO-20	91.7	63.1	1.1	68.8	1.2	30.0
2	AlSiO-10	98.8	47.9	5.6	48.5	5.7	45.8
3	AlSiO-20/B	68.6	46.0	-	67.1	-	32.9
4	AlSiO-20/L	96.3	28.9	21.9	30.0	22.7	47.3
5	Na-AlSiO-20	70.6	48.5	-	68.7	-	31.3
6	NbPO-pH2	88.2	21.5	4.6	44.6	5.2	50.2
7	Al-NbPO-pH2	95.9	38.2	12.1	39.8	12.6	47.6
8 ^[a]	AlSiO-10	90.9	41.7	1.8	45.9	2.0	52.1
9 ^[b]	AlSiO-20/B	88.5	58.6	-	66.2	-	33.8
10 ^[b]	Na-AlSiO-20	90.2	60.5	-	67.1	-	32.9
11 ^[c]	AlSiO-20/B	92.4	47.0	4.4	50.9	4.8	44.3
12 ^[d]	Al-NbPO-pH2	91.8	33.4	11.8	36.4	12.9	50.7

Reaction conditions: catalyst (0.2 g), glucose (0.2 g), water saturated with NaCl (2 ml), THF (6 ml), 160 °C, 1.5h;

[a] 2 ml 0.05 mol/L HCl instead of water; [b] reaction time: 2 h; [c] add 30 mg yttrium(III) triflate; [d] 2 ml 0.02 mol/L HCl instead of water.

Effect of the acidity on the selectivity to HMF, levulinic acid and humins

In order to address the relationship between the selectivity to HMF and by-products with the acidity of catalysts, all reactions were compared at the similar conversion level (Table 2). Detailed analysis showed that neither Lewis nor Brønsted acid sites had correlation with HMF selectivity (Figure S3), but it is very interesting to note that the weak Lewis acid sites had positive correlation with HMF selectivity; on the contrary, medium to strong Lewis acid sites had negative correlation with HMF selectivity. Therefore, in order to better understand the variation of HMF selectivity with weak Lewis acidity, HMF selectivity was plotted against the ratio of weak Lewis acidity to total Lewis acidity, a nearly linear relationship between the weak/total Lewis acid (L^*/L) ratio and the HMF selectivity was observed except at high L^*/L ratio, as present in Figure 5 a. Minimum HMF selectivity (30.0%) was achieved at the L^*/L ratio of 0.08 (Table 2, Entry 4), this was because the medium to strong Lewis acid sites could promote the formation of levulinic acid by rehydration of HMF and condensation of sugars, HMF into humins.^[13] Whereas high HMF selectivity (66.2%) was achieved over AlSiO-20/B catalyst for its high L^*/L ratio of 0.47 (Table 2, Entry 9). In order to verify the low L^*/L ratio led to the decrease of HMF selectivity, a strong Lewis acid, Yttrium trifluoroacetate [(TfO)₃Y] was added, which decreased L^*/L ratio from 0.47 to 0.25 and a significant decrease in the HMF selectivity was observed (Table 2, Entry 11), these results implied that the L^*/L ratio played important role in HMF selectivity.

Previous study^[8-10] also indicated that B/L ratio had effect on the HMF selectivity, thus, the B/L ratio with various L^*/L ratio was calculated and the correlation was present in Figure 5 b. At the similar L^*/L ratio, the HMF selectivity exhibited volcano type curve vs B/L ratio, it meant that there was a balance of Lewis and Brønsted acids for the glucose isomerization to fructose and fructose dehydration to HMF, not the higher B/L ratio, a better selectivity to HMF. Moreover, this surprising result was not only consistent with the studies reported by Ordonsky et al.,^[9,13]

where the a low B/L acid molar ratio (ca. 0.09–0.27) would promote the formation of HMF from glucose and inhibit the formation of humins, but also in agreement with the Zhang's work,^[10] where a high B/L acid molar ratio (ca. 0.72–1.85) would decrease the selectivity to HMF. At the L^*/L ratio of 0.1, the maximum HMF selectivity (39.8%) was obtained with the B/L ratio of 1.05; as the L^*/L ratio increased to 0.2-0.3, the optimum B/L ratio decreased to 0.67 for achieving the maximum HMF selectivity (50.9%). This was because as L^*/L ratio decreased, more medium to strong Lewis acids accelerated the glucose isomerization,^[9] thus high B/L ratio was desirable to speed up dehydration for achieving the maximum HMF selectivity.

While detailed analysis for by-products showed that the selectivity toward levulinic acid (LA) production from glucose decreased with the increase of L^*/L ratio, as shown in Figure 6 a and the LA selectivity exhibited volcano type curve vs B/L ratio in Figure 6 b. These results indicated the medium to strong Lewis acid sites was favourable for the selectivity to LA, which was consistent with the previous studies^[5,10] that medium to strong Lewis acid sites could drive Brønsted acid-catalyzed rehydration of HMF to formic and levulinic acids.

Figure 6 c shows the relationship of humins selectivity to L^*/L ratio and it can be found that the high L^*/L ratio leads to less formation of humins, although there was no clear quantitative correlation between the amount of Lewis acid sites and humins selectivity. Therefore the selectivity to humins was plotted against weak and medium to strong Lewis acidity and shown in Figure 6 d. It was surprisingly found that the medium to strong Lewis acidity nearly had a linear correlation with the humins selectivity under the similar B/L acid ratio (Figure S4) except at high L^*/L ratio, indicating that the medium to strong Lewis acid sites were mainly responsible for the the transformation of sugars and HMF into humins via cross-condensation.^[13] Moreover, high B/L ratio would promoted the formation of humins, revealing that the humins also generated over Brønsted acid sites, and this observation might be explained that Brønsted acid sites caused aldol addition and condensation reactions from HMF via 2,5-dioxo-6-hydroxy-hexanal(DHH).^[15]

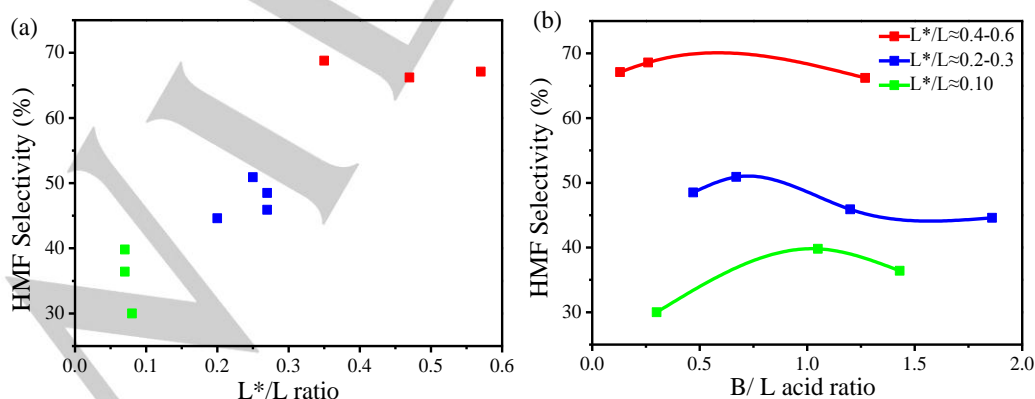


Figure 5. Effect of the L^*/L (a) and B/L (b) ratio on the selectivity to HMF. (L^*/L : weak/total Lewis acid ratio)

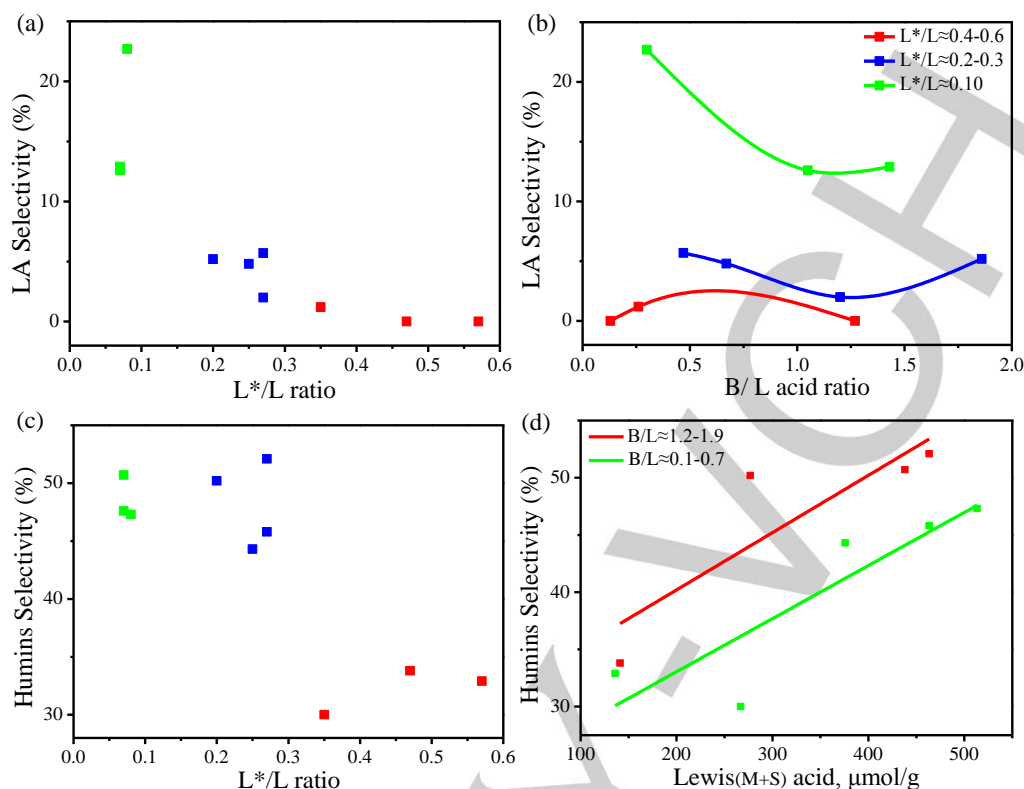


Figure 6. Effect of the L*/L (a) and B/L ratio (b) on the selectivity to LA; Effect of the L*/L (c) and medium-strong Lewis acid sites (d) on the selectivity to humins. (L*/L: weak/total Lewis acid ratio; M+S: medium+strong Lewis acid sites)

To summarize, HMF selectivity nearly had a linear correlation with the L*/L ratio, but exhibited a volcano type curve vs B/L ratio. In another hand, the medium to strong Lewis acid sites were favourable for the formation of LA and humins, thereby reducing the HMF selectivity. Similar conclusion was also drawn in lower conversions and the results are shown in Table S1 and Figure S5-7. In order to verify the above findings, NbOx sites were added to the silica-alumina composite AlSiO for acidic adjustment because of the hydrothermal stability of Nb₂O₅,^[16] then used in conversion of glucose to HMF.

Niobium doped AlSiO for high selectivity to HMF with acidic adjustment.

The X-ray powder diffraction patterns of various Nb-AlSiO materials indicated that all the Nb-AlSiO samples were amorphous, as shown in Figure S8, and no crystalline Nb₂O₅ phase was detected in Nb-AlSiO samples, indicating that the amorphous niobium oxide species were well dispersed. All Nb-AlSiO materials were mesoporous from Nitrogen adsorption-desorption isotherms (Figure S9), and the representative sample of Nb_{0.15}Al_{0.85}Si₂₅O had the surface area of 766.2 m²g⁻¹ and pore volume of 0.50 cm³g⁻¹ (Table S2). To study the amount of the acid sites of Nb-AlSiO materials, the NH₃-TPD was measured and shown in Figure S10. All samples had broad peaks in the range of 100-500 °C, indicating the presence of

weak, medium to strong acid sites. The total amount of the acid sites determined by NH₃-TPD increases in the following order: Nb_{0.15}Al_{0.85}Si₂₅O < Nb_{0.30}Al_{0.70}Si₂₅O < Nb_{0.40}Al_{0.60}Si₂₅O, revealing the increase of the Nb/Al ratio lead to the increase of the total acid sites.

To investigate the types and strength of acidic sites, the Py-FTIR spectra were recorded in Figure S11. The amounts of Brønsted and Lewis acid sites on various mesoporous Nb-AlSiO catalysts were quantified and summarized in Table 4. Both the amounts of Brønsted and Lewis acid sites increased with increasing Nb/Al ratio, especially for Brønsted acid sites, the B/L acid ratio increased from 0.68 to 0.87, while the L*/L acid ratio increased from 0.40 to 0.49. The Nb_{0.40}Al_{0.60}Si₂₅O sample had the larger acidity (718 μmol g⁻¹) than other samples, which was in agreement with the results of NH₃-TPD (Figure S10).

The Nb-AlSiO catalysts had similar L*/L acid ratio with that of AlSiO-20 catalyst, and the B/L ratio increased in the following order: AlSiO-20 < Nb_{0.15}Al_{0.85}Si₂₅O < Nb_{0.30}Al_{0.70}Si₂₅O < Nb_{0.40}Al_{0.60}Si₂₅O, then the HMF selectivity decreased in the following order: Nb_{0.15}Al_{0.85}Si₂₅O > AlSiO-20 > Nb_{0.30}Al_{0.70}Si₂₅O > Nb_{0.40}Al_{0.60}Si₂₅O under the similar glucose conversion (Table 2 and Table 5). This result can be explained from Figure 5 b, the B/L ratio (0.68) of Nb_{0.15}Al_{0.85}Si₂₅O is more suitable than others in terms of the selectivity to HMF, and higher B/L ratio (0.87) of Nb_{0.40}Al_{0.60}Si₂₅O may lead to more unselective glucose, fructose

Table 4. The amounts of Brønsted and Lewis acid sites on various catalysts by Py-FTIR.

Entry	Cata	Acid from Py-FTIR ($\mu\text{mol g}^{-1}$)											
		Brønsted				Lewis				Total	B/L	B*/B	L*/L
		W	M	S	Total	W	M	S	Total				
1	Nb _{0.15} Al _{0.85} Si ₂₅ O	28	63	98	189	112	93	74	279	468	0.68	0.15	0.40
2	Nb _{0.30} Al _{0.70} Si ₂₅ O	39	79	114	232	146	80	92	318	550	0.73	0.17	0.46
3	Nb _{0.40} Al _{0.60} Si ₂₅ O	70	92	172	334	188	89	106	383	717	0.87	0.21	0.49

W: weak acid sites; M: medium acid sites; S: strong acid sites;
 B*/B: weak /total Brønsted acid sites;
 L*/L: weak /total Lewis acid sites;

Table 5. Summary of the glucose conversion, HMF yield and selectivity, LA yield and selectivity and humins selectivity catalyzed by various catalysts

Entry	Catalyst	C _{glucose} /%	Y _{HMF} /%	Y _{LA} /%	S _{HMF} /%	S _{LA} /%	S _{humins} /%
1	Nb _{0.15} Al _{0.85} Si ₂₅ O	80.8	57.8	0.3	71.5	0.4	28.1
2	Nb _{0.30} Al _{0.70} Si ₂₅ O	82.2	55.9	0.7	68.0	0.9	31.1
3	Nb _{0.40} Al _{0.60} Si ₂₅ O	87.7	51.4	0.7	58.6	0.8	40.6
4 ^[a]	Nb _{0.15} Al _{0.85} Si ₂₅ O	92.6	65.7	0.7	71.0	0.8	28.2
5 ^[a]	Nb _{0.30} Al _{0.70} Si ₂₅ O	95.4	65.3	1.0	68.5	1.0	30.5
6 ^[a]	Nb _{0.40} Al _{0.60} Si ₂₅ O	97.7	56.0	1.3	57.3	1.3	41.4

Reaction conditions: catalyst (0.2 g), glucose (0.2 g), water saturated with NaCl (2 ml), THF (6 ml), 160 °C, 1.5 h;

[a] reaction time: 2 h.

or HMF condensation into humins, resulting in a low HMF selectivity.[15]

The results obtained over the Nb-AlSiO samples well confirmed above findings, the excellent performance of the solid acid catalysts with high selectivity to HMF requires the higher L*/L ratio and suitable B/L ratio. The recyclability and stability of Nb_{0.15}Al_{0.85}Si₂₅O catalyst was investigated by reusing the catalyst in consecutive catalytic runs and the results are presented in Figure 7. It can be seen that the glucose conversion and HMF yield were still maintained at 61.4% and 41.3%, respectively, indicating its good stability.

Conclusions

The selective formation of HMF from glucose has been studied using silica-alumina composite (AlSiO) catalysts and the effect of acidity on the catalytic activity and selectivity were systematically investigated. The results shows that Lewis acid sites promotes glucose conversion, whereas Brønsted acid sites not only has detrimental effect on glucose conversion, but also promotes aldol addition and condensation reaction from HMF; HMF selectivity nearly had a linear correlation with the L*/L ratio, and exhibited a volcano type curve vs B/L ratio; weak Lewis acid sites promotes HMF production, while the medium to strong Lewis acid sites is responsible for the undesired by-products (LA, humins) formation. Then, niobium-doped mesoporous AlSiO as

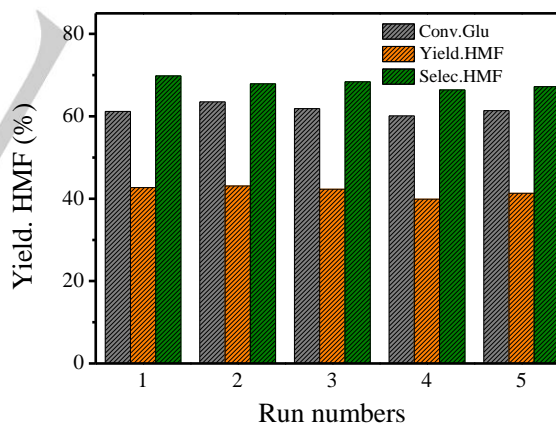


Figure 7. Cycle usage of Nb_{0.15}Al_{0.85}Si₂₅O catalyst. (Reaction conditions: 0.2 g Nb_{0.15}Al_{0.85}Si₂₅O catalyst, 0.2 g glucose, 2 ml water saturated with NaCl, 6 ml THF, 160 °C, 1.5 h.)

a catalyst, showed good recycle performance and well verified the above findings for its excellent performances on catalytic activity and selectivity, and highest HMF selectivity (71%) was achieved over Nb_{0.15}Al_{0.85}Si₂₅O catalyst. This work can help to design acid catalysts with suitable amount and strength to achieve the ideal goal for producing HMF from glucose or other carbohydrates.

Experimental Section

Materials

5-Hydroxymethylfurfural (HMF) were purchased from Alfa Aesar Chemical Reagent Company. All chemicals were purchased from Sinopharm Chemical Reagent Co. Ltd. Nb tartrate was prepared in our laboratory according to the literature.^[10] Tetrahydrofuran (THF) was chemical pure solvent and purchased from shanghai chemicals company. All bought chemicals were of analytical grade and used without further purification.

Catalyst preparation

AlSiO-10, AlSiO-20 samples was synthesized according to the literature.^[11] The preparation of Nb-AlSiO was similar to that of AlSiO except extra addition of niobium tartrate before the addition of TEOS.

AlSiO-20/B was obtained by using TEOS as the silylation agent. 1g of dried AlSiO-20 catalyst was added to a solution of 1 g of TEOS in 25 mL of n-hexane. The mixture was stirred at room temperature for 12 h. AlSiO-20/L prepared by the above and calcination (823K) for further 4 h. Na-AlSiO-20 sample was obtained by ion-exchange of AlSiO-20 sample with NaCl. In details, 3.0 g of AlSiO-20 sample was stirred in 300 mL of 0.2 M NaCl solution, and the mixture was maintained at pH = 5.5 by adding 0.05 M NaOH solution. After 24 h, the collected sample was washed repeatedly with distilled water until Na⁺ and Cl⁻ ions were no longer detected, and then dried at 373 K for 24 h.

Mesoporous niobium phosphate catalysts NbPO and Al-NbPO were prepared according to our previous work.^[10]

Characterization

Powder XRD patterns were recorded on a Bruker diffractometer (D8 Focus) by using Cu K α ($\lambda=0.154056$ nm) radiation. Nitrogen adsorption-desorption isotherms were measured at -96 °C on a NOVA 4200e analyzer (Quantachrome Co. Ltd). Before the measurements, all samples were outgassed at 180 °C for 12 h under vacuum to remove moisture and volatile impurities. The BET method was used to calculate the specific surface area. Pore size distribution curves were derived from the desorption branches of the isotherms and calculated by the Barrett-Joyner-Halanda (BJH) method. The total pore volume (V_t) was estimated at a relative pressure of 0.975.

Ammonia temperature-programmed-desorption (NH₃-TPD) was carried out in a PX200 apparatus (Tianjin Golden Eagle Technology Limited Corporation) with a thermal conductivity detector (TCD). The catalyst (100 mg) was charged into the quartz reactor, and the temperature was increased from room temperature to 600 °C at a rate of 10 °C min⁻¹ under a flow of N₂ (40 ml min⁻¹), and then the temperature was decreased to 90 °C. Finally, NH₃ was injected into the reactor at 90 °C under a flow of N₂ (40 ml min⁻¹). When the adsorption saturation was reached, followed by a flow of N₂ for 1h at 90 °C, then the temperature was increased from 90 °C to 600 °C at a rate of 10 °C min⁻¹ and the amount of desorbed ammonia was detected by using

thermal conductivity detector (TCD) at 110 °C. Besides, a blank measurement was conducted without adsorption of ammonia and after deducted the blank measurement, the NH₃-TPD curve of catalysts were obtained.

Infrared (IR) spectra of pyridine adsorption were recorded on Nicolet NEXUS 670 FT-IR spectrometer. The samples were pressed into self-supporting disks and placed in an IR cell attached to a closed glass-circulation system. The disk was dehydrated by heating at 400 °C, for 1 h under vacuum in order to remove physic-sorbed water. After the cell was cooled to room temperature, the IR spectrum was recorded as background. Pyridine vapor was then introduced into the cell at room-temperature until equilibrium was reached, and then a second spectrum was recorded. Subsequent evacuations were performed at 100, 200 and 400 °C, for 10 min followed by spectral acquisitions. The spectra presented were obtained by subtracting the spectra recorded before and after pyridine adsorption.

The quantification of acid sites was performed using the same expressions as those in the research article of Rocha *et al.*:^[12]

$$C_L = K_L \times A_{1440} = \frac{\pi}{IMEC_L} \times \left(\frac{r^2}{w}\right) \times A_{1450}$$

and

$$C_B = K_B \times A_{1540} = \frac{\pi}{IMEC_B} \times \left(\frac{r^2}{w}\right) \times A_{1540}$$

C_L and C_B are the concentrations of Lewis acid sites and Brønsted acid sites in $\mu\text{mol g}^{-1}$; A_{1450} and A_{1540} are the integrated areas of bands at 1450 and 1540 cm^{-1} in the original data of FTIR spectra, as shown in the Results and discussion section. K_L and K_B are molar extinction constants for Lewis and Brønsted acid sites; $IMEC_L$ and $IMEC_B$ are integration molar extinction coefficients, 2.22 and 1.67 $\text{cm} \mu\text{mol}^{-1}$ for Lewis and Brønsted acids, respectively; r is the wafer radius in cm and w is the wafer weight in g of the self-supporting catalyst disk.

Catalytic reactions

The influence of external diffusion can be totally eliminated by changing stirring speed. It is found that stirring speed had no influence on the catalytic performance if stirring speed was above 300 rpm. The influence of the internal diffusion can be eliminated by decreasing the particle size of catalyst, the catalyst size had no effect on the conversion of glucose if the size was lower than 150 μm .^[11] All the dehydration reaction experiments were conducted in a Teflon-lined stainless steel autoclave (30 ml) equipped with a temperature-controlled heating-jacket and a magnetic stirrer, then the mixture was stirred at 700 rpm to guarantee that it is properly stirred. The mixture of carbohydrate, solvent (6 mL organic phase and 2 mL H₂O saturated with NaCl) and 0.2 g catalyst (the particle size of catalysts are the same and lower than 150 μm) were put in the sealed autoclave. 0.5 M Pa N₂ gas was used for purging air outside the reactor and keeping solvent in liquid phase. When the reactor was raised to the desired temperature, zero time was

recorded. Then, the reactor was held at this temperature for a given period of time. After reaction, the autoclave was cooled to room temperature by loading cooling water. The solid catalyst was removed by filtration, and the filtrate was taken for analysis. During the recycling, the upper organic phase was removed after the reaction and the catalyst kept in the aqueous phase was used directly in the next cycle with separation, washing and drying.

Product analysis

The analysis of HMF was carried out by means of an HPLC apparatus (Agilent 1200 Series) equipped with an XDB-C18 column (Eclipse USA) and quantified with an ultraviolet detector (Agilent G1314B) at 254 nm based on the external standard. The eluent with a flow rate of 0.6 mL min⁻¹ was a mixture of methanol and water with volumetric ratio of 20:80. An auto-sampler (Agilent G1329A) was used to enhance the reproducibility. Glucose, fructose, and levulinic acid (LA) were analyzed with a refractive index detector (Agilent G1362A) and using a Biorad Aminex HPX-87H sugar column at 328K. The mobile phase was 0.004 M H₂SO₄ with a flowing rate of 0.45 mL min⁻¹.

Conversion of glucose and yield of HMF and levulinic acid were defined as follows:

$$\text{Glucose conversion} = \frac{\text{moles of glucose reacted}}{\text{moles of starting glucose}}$$

$$\text{HMF yield} = \frac{\text{moles of HMF produced}}{\text{moles of starting glucose}}$$

$$\text{Levulinic acid yield} = \frac{\text{moles of levulinic acid produced}}{\text{moles of starting glucose}}$$

Acknowledgements

This work was supported financially by the NSFC of China (No. 91545103, 21273071 and 21403065) and the Science and Technology Commission of Shanghai Municipality (10dz2220500).

Keywords: glucose conversion; 5-hydroxymethylfurfural; Lewis acid sites; B/L ratio

- [1] a) Y. Román-Leshkov, C. J. Barrett, Z. Y. Liu and J. A. Dumesic, *Nature*. **2007**, 447, 982-985; b) P. Gallezot, *Chem. Soc. Rev.* **2012**, 41, 1538-1558; c) C. H. Zhou, C. X. Lin, D. S. Tong and J. beltrami. *Chem. Soc. Rev.* **2011**, 40, 5588-5617; d) J. J. Bozell and G. R. Petersen, *Green Chem.* **2010**, 12, 539-554.
- [2] a) J. J. Wang, J. W. Ren, X. H. Liu, G. Z. Lu and Y. Q. Wang, *AIChE Journal*. **2013**, 59, 2558-2566; b) J. J. Wang, W. J. Xu, J. W. Ren, X. H. Liu, G. Z. Lu and Y. Q. Wang, *Green Chem.* **2011**, 13, 2678-2681; c) P. Gallezot, *Chem. Soc. Rev.* **2012**, 41, 1538-1558; d) A. Rosatella, S. P. Simeonov, R. F. M. Frade and C. A. M. Afonso, *Green Chem.* **2011**, 13, 754-793.
- [3] a) H. Huang, C. A. Denard, R. Alamillo, A. J. Crisci, Y. Miao, J. A. Dumesic, S. L. Scott, and H. Zhao, *ACS Catal.* **2014**, 4, 2165-2168; b) M. Moliner, Y. Román-Leshkov and M. E. Davis, *Proc. Natl. Acad. Sci. U. S. A.* **2010**, 107, 6164-6168; c) R. O. L. Souza, D. P. Fabiano, C. Feche, F.

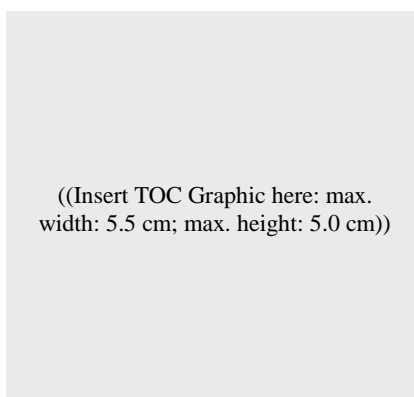
- Rataboul, D. Cardoso, N. Essayem, *Catalysis Today*. **2012**, 195, 114-119.
- [4] Y. Román-Leshkov, M. Moliner, J. A. Labinger, and M. E. Davis, *Angew. Chem. Int. Ed.* **2010**, 49, 8954-8957.
- [5] a) T. M. C. Hoang, E. R. H. van Eck, W. P. Bula, J. G. E. Gardeniers, L. Lefferts and K. Seshan, *Green Chem.* **2015**, 17, 959-972; b) B. Saha and M. M. Abu-Omar, *Green Chem.* **2014**, 16, 24-38.
- [6] H. Nguyen, V. Nikolakis, D. G. Vlachos, *ACS Catal.* **2016**, 6, 1497-1504.
- [7] Y. P. Li, M. H. Godon, and A. T. Bell, *ACS Catal.* **2014**, 4, 1537-1545.
- [8] V. V. Ordonsky, V. L. Sushkevich, J. C. Schouten, J. van der Schaaf, T. A. Nijhuis, *J. Catal.* **2013**, 300, 37-46.
- [9] T. Dallas Swift, H. Nguyen, Z. Erdman, J. S. Kruger, V. Nikolakis, D. G. Vlachos, *J. Catal.* **2016**, 333, 149-161.
- [10] a) Y. Zhang, J. J. Wang, J. W. Ren, X. H. Liu, X. C. Li, Y. J. Xia, G. Z. Lu, Y. Q. Wang, *Catal. Sci. Technol.* **2012**, 2, 2485-2491; b) Y. Zhang, J. J. Wang, X. C. Li, Y. J. Xia, B. C. Hu, G. Z. Lu, Y. Q. Wang, *Fuel* **2015**, 139, 301-307; c) D. Q. Ding, J. X. Xi, J. J. Wang, X. H. Liu, G. Z. Lu, Y. Q. Wang, *Green Chem.* **2015**, 17, 4037-4044.
- [11] X. C. Li, Q. N. Xia, V. C. Nguyen, K. H. Peng, X. H. Liu, N. Essayem and Y. Q. Wang, *Catal. Sci. Technol.* DOI: 10.1039/c6cy01628f.
- [12] A. S. Rocha, A. M. S. Forrester, M. H. C. de la Cruz, C. T. da Silva and E. R. Lachter, *Catal. Commun.* **2008**, 9, 1959-1965.
- [13] a) V. V. Ordonsky, J. V. D. Schaaf, J. C. Schouten, and T. A. Nijhuis, *ChemSusChem*. **2013**, 6, 1697-1707; b) V. V. Ordonsky, J. V. D. Schaaf, J. C. Schouten, and T. A. Nijhuis, *ChemSusChem*. **2012**, 5, 1812-1819.
- [14] S. Zheng, H. R. Heydenrych, A. Jentys, J. A. Lercher, *J. Phys. Chem. B.* **2002**, 106, 9552-9558.
- [15] S. K. R. Patil, C. R. F. Lund, *Energy Fuels*. **2011**, 25, 4745-4755.
- [16] K. Nakajima, Y. Baba, R. Noma, M. Kitano, J. N. Kondo, S. Hayashi and M. Hara, *J. Am. Chem. Soc.* **2011**, 133, 4224-4227.

Entry for the Table of Contents (Please choose one layout)

Layout 1:

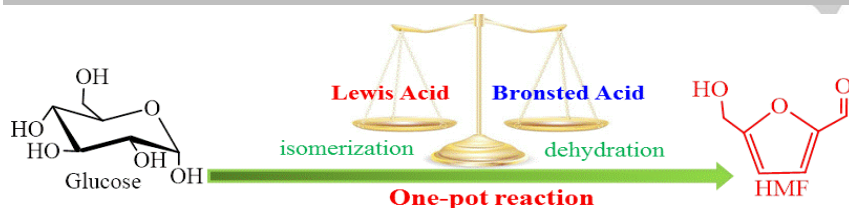
FULL PAPER

Text for Table of Contents

*Author(s), Corresponding Author(s)****Page No. – Page No.****Title**

Layout 2:

FULL PAPER

*Xiangcheng Li, Kaihao Peng, Xiaohui Liu*, Qineng Xia, Yanqin Wang****Page No. – Page No.****Comprehensive Understanding the Role of Brønsted and Lewis Acid Sites in Glucose Conversion to 5-Hydromethylfurfural**

The selective formation of HMF from glucose has been studied using silica-alumina composite (AlSiO) catalysts, and the effect of Brønsted and Lewis acid sites on the catalytic activity and selectivity was systematically investigated.